The use of multi-wall carbon nanotube for improving the mechanical performance of epoxy resin based metal oxide hybrid nanocomposites

Bakhan S. Mustafa
Gelas M. Jamal
Omed Gh. Abdullah (omed.abdullah@univsul.edu.iq)
University of Sulaimani https://orcid.org/0000-0002-1914-152X

Research Article

Keywords: nanocomposite materials, multi-wall carbon nanotube, metal oxide nanoparticles, epoxy resin, mechanical properties

Posted Date: June 2nd, 2022

DOI: https://doi.org/10.21203/rs.3.rs-1674755/v1

Abstract

This study aims to explore the improvement in the mechanical characterization of epoxy resin (EPR) based hybrid nanocomposite, reinforced with multi-wall carbon nanotube (MWCNT), zirconium dioxide (ZrO_2), and yttrium oxide (Y_2O_3) nanoparticles (NPs). The intercalation behavior of the fillers in the composites was studied by monitoring the change of X-ray diffraction (XRD) patterns. The effect of different components on tensile properties of filled EPR PNCs was investigated. Results show that there was a remarkable improvement in the mechanical properties of hybrid nanocomposites at small loading levels of MWCNT. The addition of MWCNT at 0.1 has increased the composite Young's modulus, 28.38% in comparison with pure EPR. The reduction of elongation at break for EPR upon incorporating MWCNT is due to the high agglomerates of MWCNT in the PNCs. The low-weight fraction of CNTs (0.1 wt.%) was found to be effective in enhancing the toughness by 18.13% in comparison to pure EPR. Furthermore, the optimized hybrid EPR reinforced MWCNT shows a higher Young's modulus value of 2492.06 MPa upon loading 1 wt.% NPs. The reduction of the tensile strength of the EPR PNCs is due to NPs agglomeration. The present study illustrates that the mechanical and structural properties of bulk EPR can be tailored by incorporating a very low nano-fillers concentration.

1. Introduction

Polymer nanocomposites (PNCs) have drawn intense attention from scientists working in various disciplines due to significant improvement in the performance of the composites because of the structure, surface area, and side effects of nanoparticles (NPs) [1, 2]. Carbon nanotubes (CNTs) are commonly employed as reinforcements in polymeric matrices to form PNCs due to an exceptionally high aspect ratio and low density, as well as high strength and stiffness. [3, 4]. CNTs are an allotrope of carbon that can be classified depending on the number of graphene walls in their structure into single walled (SW-), double walled (DW-), and multi walled (MW-) CNTs [5]. It has been well reported that the low loading of CNTs improves the PNCs strength by as much as 25% [6]. The dispersion quality of the CNTs and the interfacial adhesion between the polymer host and the CNTs are the two most important aspects of optimizing the reinforcing effects of CNTs in PNCs [7–9]. Because of their high aspect ratio and strong van der Waals attraction, CNTs typically form agglomerates, resulting in inhomogeneous dispersion in polymer matrices [10]. Pras et al. [11], reported that the CNT dispersion state has an outstanding effect on the CNT releasing potential in the PNCs, the mechanical properties were enhanced when the carbon nanotubes are well dispersed. The improvements in the properties of homogeneously dispersed CNTs in PNCs come from interactions at the molecular scale between CNTs and host polymer chains, influencing the physical and material properties of the host matrix [12].

PNCs, on the other hand, have superior mechanical and physical properties over the host pure resin partially due to the large interfacial area between NPs and resin, which produced some unexpected properties not found in conventional polymer composites. [13]. Generally, there are three basic mechanisms of interfacial load transfer between the host matrix and the reinforcement phase, which are micro-mechanical interlocking, strong chemical bonding, and weak van der Waals bonding [14, 15].

Epoxy resin (EPR) is the most popular thermosetting material, having epoxide groups on its molecules [16]. EPR nanocomposites are widely used in many sectors such as electronics, civil, marine, and aerospace industries, because of their low cost, super adhesiveness, lightweight, excellent corrosion resistance, and minimum shrinkage during curing [17, 18]. Numerous studies have been conducted to explore the mechanical toughness of EPR composites [19–21]. Inorganic additives, such as silica (SiO_2) and alumina (Al_2O_3) have been used to enhance the toughness of EPR without sacrificing their basic properties, but the presence of high loading inorganic particles increases the apparent viscosity of the matrix, resulting in poor dispersion and processing difficulties [22, 23]. Saravanan et al. [24], reported that the alumina particles in hybrid EPR PNCs act as 'chariot' for the CNTs to homogenous dispersion and improve the host matrix synergetic properties. In this study, the mechanical properties of EPR based hybrid nanocomposite reinforced with low concentrations of MWCNT, zirconium dioxide (ZrO_2), and yttrium oxide (Y_2O_3) NPs have been investigated. This research aims to obtain the optimal composition of hybrid PNCs with a maximum level of mechanical properties, to be applicable in diverse applications. To ensure the high disperse of NPs within the epoxy matrix, high-power sonication was used.

2. Experimental Details

Commercial epoxy resin (EPR) (Quick-mast 105) produced by Don Construction Products was used as a host matrix, and Polyoxypropylenediamine provided by the same company was used as the hardener or curing agent. Multi-wall carbon nanotube (MWCNT) with purity > 99 wt.%, outer diameter 13–18 nm, and length 3–30 μm, is purchased from Cheap Tubes Inc. The high purity zirconium dioxide (ZrO_2), and yttrium oxide (Y_2O_3) NPs both with a particle size of 50 nm were purchased from Merck Company. All the additives were used as reinforcement for hybrid PNCs.

Different EPR PNCs were prepared by incorporating MWCNT with concentrations of 0.1 and 0.2 wt.%, and a mixture of ZrO_2/Y_2O_3 NPs with concentrations of 0.25, 0.50, 0.75, 1.0, 1.25, and 1.5 wt.%. The high shear-mixing and ultrasonic methods were used to achieve high homogeneous dispersion of NPs throughout EPR. This process caused a reduction in EPR viscosity and NPs aggregate size. Air bubbles were eliminated by placing the PNC samples in a vacuum for 45 minutes, followed by adding a fixed amount of hardener in the volume ratio of 1:3 and stirring the mixture for 2 min. The obtained viscous homogeneous solution was then slowly cast into the appropriate molds according to ASTM standards to get the desired shape for mechanical testing. After consolidation at room temperature for 24 hours, the samples were cured in the oven at 70°C for 4 hours to remove the moisture contents and to reduce the residual stresses formed through the hardening process. The cross-linked structures formed during the curing process. The schematic diagram of the preparation stages of the EPR nanocomposites is elucidated in Fig. 1. The dimensions of dog-bone and rectangular specimens of pure EPR and that of the PNCs are illustrated in Fig. 2.

The tensile test and three-point bending test were conducted to characterize the mechanical properties of the prepared nanocomposites. The bending and tensile tests were conducted according to ASTM D790

and ASTM D638-02a, respectively, on a Testometric universal testing machine with a 100 kN maximum load. The loading rate for the tensile test was 10 mm/min, while for the bending test the load was applied at a rate of 5.3 mm/min perpendicular to the sample. The span between two supports in a three-point-bending fixture was 80 mm as shown in Fig. 2-a. WinTest analysis universal testing software was utilized to control testing. A minimum of five samples were tested for each PNC and the average values were reported. It should be noted that the toughness value of each specimen was calculated using numerical integration based on the trapezoid method.

The change in the structural properties of EPR upon incorporating different fillers was studied using X-ray diffraction (XRD) with X'pert PRO PANalytical diffractometer equipped with a Cu-Ka radiation (λ = 1.5406 Å) operated at 45 kV and 40 mA. The scanning speed and step sizes were 1°/min and 0.1°, respectively. The diffraction patterns were collected over generated angles between 5° and 75°.

3. Results And Discussion

3.1 MWCNT reinforced EPR

The tensile tests were conducted to determine the tensile strength, modulus of elasticity, and toughness of the system. The tensile stress-strain curves for pure EPR and EPR reinforced MWCNT is presented in Fig. 3. We can note the increase in the stress of PNCs upon incorporating MWCNT concentrations, whereas the strain is reduced for both components. The stress-strain curves of the PNCs specimen incorporated 0.2 wt.% MWCNT reveal rather brittle compared to other specimens, which could be due to agglomerations of the MWCNTs due to the van der Waals attraction between adjacent nanotubes. The agglomerations and entangle of CNTs in different PNCs have been reported by many researchers [25, 26]. Wang et al. [27] reported that the aggregation of CNTs has a negative effect on the synchronous enhancement of the PNCs. The tensile stress-strain curve was used to derive some of the most important mechanical properties such as ultimate tensile strength, elongation at break, Young's modulus, and toughness of the present system.

The average ultimate tensile strength and the elongation at break for pure EPR and its PNCs reinforced with MWCNT were shown in Fig. 4. The values plotted are the average of at least five specimens tested, and the error bars show the standard deviation error for each PNC. The ultimate strength of EPR was increased upon incorporating MWCNT. The maximum tensile strength was observed to be 48.87 MPa for the EPR/0.1 MWCNT sample, increasing around 23% in comparison to pure EPR (39.73 MPa), which may be attributed to the interlocking mechanism between MWCNTs and EPR matrix [28]. The further increase in the MWCNT contents leads to a reduction in the tensile strength of PNCs due to the possibility of MWCNT agglomerations in the matrix. On the other hand, the elongation at break of EPR decreased gradually with increasing MWCNT contents, leading to a decrease in the toughness of the matrix. Zakaria et al. [29], also found that adding both graphene nanoparticles (GNP) and MWCNT to EPR made it more brittle, resulting in a reduction in the elongation at break.

Figure 5 displays the variation of Young's modulus, and toughness (area under the stress-strain curve) of EPR PNCs reinforced with MWCNTs. Young's modulus of EPR increases with increasing MWCNT contents. These increases are 28.38% and 19.08% upon the addition of 0.1 and 0.2 wt.% of MWCNT in the resin, respectively. A strong interaction between the nano-fillers and the polymer matrix even at low filler loading conditions may be responsible for this improvement in tensile properties. Salah et al. [30] also reported an increase in Young's modulus and a decrease in elongation at break for polycarbonate reinforced with low-weight fractions of CNTs.

The higher average toughness was achieved for the EPR/0.1 MWCNT sample, by increasing around 18.13% in comparison to pure EPR. This improvement is explained due to the good dispersion of MWCNT in the composite at this loading, which provides an effective load transfer from the EPR matrix to MWCNT [29]. The reduction of the toughness of the EPR/0.2 MWCNT sample is most likely owing to a decrease in the elongation at break as a result of the agglomerations of MWCNTs as depicted in Fig. 4. The aggregations and agglomerations of MWCNT limit the load transfer from the matrix to the additives.

The effect of adding MWCNT on the bending strength at a peak, bending strain at a break, and bending modulus were also studied using the 3-point bending test. Table 1 tabulated all these parameters for pure EPR and its PNCs reinforced with different concentrations of MWCNT. It was found that the addition of 0.1 wt.% MWCNT significantly improves the bending strength and bending modulus compared to pure EPR.

Table 1
Bending strength at a peak, bending strain at a break, and bending modulus for pure EPR and its PNCs reinforced with MWCNT.

MWCNT wt.%	Bending strength at a peak (MPa)	Bending strain at a break (mm)	Bending modulus (MPa)
0	81.91 ± 1.28	17.83 ± 1.23	2716.87 ± 59.07
0.1	95.29 ± 1.91	15.57 ± 2.13	3128.86 ± 60.93
0.2	94.92 ± 0.87	12.14 ± 3.20	3055.40 ± 47.54

The reduction in bending strain at break of the reinforced EPR was also observed in the previously published studies for different fillers incorporated in the EPR matrix. Rostam et al. [31] studied the bending properties of EPR incorporated with different content of $CaTiO_3$ NPs. They also reported a reduction in the deflection at peak and an increase in the flexural strength at a peak. The further increasing the MWCNT content caused a reduction in bending properties, which is probably due to the agglomerate formation [32].

X-ray diffraction (XRD) analysis was performed to determine the structural characteristics of EPR reinforced MWCNT. The XRD patterns for pure EPR and its PNCs reinforced with MWCNT are shown in Fig. 6. The presence of two broad diffraction peaks at around 20° and 43° indicates that the cured EPR matrix is amorphous in nature. The XRD patterns for PNCs reinforced with MWCNT exhibit the

broadening in the characteristic peaks of EPR and a decrease in their intensity indicating the intercalation of MWCNT between EPR matrix, which significantly influences the mechanical properties of the matrix [33]. The XRD pattern for EPR reinforced 0.1 wt.% MWCNT exhibits moderate interactions between the MWCNTs and EPR matrix, as a consequence of the reduction in the XRD peaks intensity, thus the addition of 0.1 wt.% of MWCNT to EPR provides the mechanism for stress transfer at the interface between MWCNTs and EPR that is manifest in the large increases in the mechanical properties of this compound. McClory et al. [34], also demonstrated that the addition of just 0.1 wt.% MWCNTs in polyurethane resulted in significantly enhanced stiffness, strength, and toughness of the matrix due to strong interfacial shear stress between MWCNTs and polyurethane chains.

3.2 Hybrid EPR PNCs

In order to investigate the influence of ZrO_2 and Y_2O_3 NPs contents as well as MWCNTs on the tensile strength, a series of specimens with the same processing condition but different NPs weight percent were prepared and tested. The typical stress-strain curves under tensile loading for all hybrid EPR PNC systems are shown in Fig. 7. We can see that the tensile strength increases significantly with the increasing amounts of NPs contents for hybrid PNCs in comparison to pure EPR.

Figure 8 depicted the graphical representation of the effect of NPs contents on the ultimate strength, elongation at break, and Young's modulus for all hybrid EPR PNCs. The ultimate tensile strength of EPR PNCs and its MWCNT hybridization for all compositions show a considerable improvement compared to the neat EPR. It is observed that EPR incorporated 1 wt.% NPs in the presence of 0.1 CNT exhibit higher ultimate tensile strength with a value of 48.92 MP, which is 23.12% higher than that of neat EPR.

The elongation at break of hybrid EPR PNCs with different NPs loadings is shown in Fig. 8-c. It is clearly seen that the values of elongation at break for all composites decreased with NPs loading. Indicating that the hybrid EPR PNCs become more brittle in comparison to neat EPR. On the other hand, it is interesting to note that the hybrid EPR PNCs exhibit improved tensile Young's modulus for all compositions. The EPR incorporated 0.75 ZrO_2 and 0.75 Y_2O_3 has a 35.14% higher Young's modulus compared to pure EPE which is 1819.87 MPa. Whereas the hybrid EPR/0.1 MWCNT/1 wt.% NPs show an improved tensile modulus of 33.66% higher than the pure EPR. The improvement in the tensile modulus is due to the homogeneous dispersion of NPs at that concentration and the stress transfer of MWCNTs. However, the further addition of NPs reduces the tensile strength and tensile modulus for all hybrid PNCs. Many researchers have reported this phenomenon, due to the agglomeration of fillers in the host polymer matrix due to difficulties in the dispersion of higher filler loading [24]. Uddin and Sun [35] investigated the mechanical properties of hybrid silica/alumina/carbon nanofibers (CNF)/epoxy composites. They concluded that the particle dispersion in the resin is the dominant factor in deciding the amount of enhancement in the mechanical properties of the system.

The toughness of the hybrid EPR PNCs is derived from the stress-strain curves and the results were presented in Fig. 9. It is interesting to note that hybrid systems EPR + ZrO_2 + Y_2O_3 and EPR + 0.1CNT + ZrO_2 + Y_2O_3 exhibit maximum toughness when loaded, respectively, with 0.5 and 1 wt.% NPs. The highest

value for tensile toughness of $161.85 \cdot 10^4$ J.m^{-3} was achieved for EPR + ZrO_2 + Y_2O_3 nanocomposites, which may be due to the homogeneous stress distribution between the host EPR matrix and fillers. On the other hand, failure occurred for some weight fractions of the hybrid EPR PNCs that were unable to transfer the stress during loading due to agglomeration of fillers as reported by many researchers [36, 37].

The bending properties for hybrid EPR/0.1 MWCNT/ZrO_2/Y_2O_3 PNCs with different NPs contents are presented in Table 2. It is evident that the highest bending strength at a peak, bending strain at a break, and bending modulus was achieved by incorporating 0.5 wt.% NPs. The highest bending strength of the hybrid EPR/0.1 MWCNT/ZrO_2/Y_2O_3 PNCs was 91.02 MPa, which presented an enhancement of up to 11% compared to pure EPR. Meanwhile, the increment in bending strain at a break was 19.74% compared to the pure EPR.

Table 2
Bending strength at a peak, bending strain at a break, and bending modulus for hybrid EPR/0.1 MWCNT/ZrO_2/Y_2O_3 PNCs with different NPs contents.

NPs wt.%	Bending strength at a peak (MPa)	Bending strain at a break (mm)	Bending modulus (MPa)
0.00	95.29 ± 1.91	15.57 ± 1.59	3128.86 ± 60.93
0.25	87.54 ± 0.47	17.13 ± 0.36	2604.38 ± 9.27
0.50	91.02 ± 1.55	21.36 ± 0.50	2835.85 ± 19.00
0.75	82.76 ± 1.47	16.35 ± 0.99	2496.82 ± 61.34
1.00	82.23 ± 2.89	16.05 ± 0.32	2438.80 ± 75.25
1.25	79.78 ± 0.17	20.46 ± 0.66	2492.07 ± 9.54
1.50	84.04 ± 1.47	19.56 ± 0.30	2766.01 ± 37.50

Figure 10 depicted the XRD patterns for hybrid EPR PNCs with different concentrations of NPs (ZrO_2 and Y_2O_3). The NPs addition caused a broadening and decrease in the intensity of the EPR characterization peaks indicating intercalation of NPs in the resin [33]. Moreover, incorporating NPs in the hybrid PNCs leads to the appearance number of new sharp diffraction peaks in the XRD patterns, their intensity increases with increasing NPs contents.

The crystalline peaks found in 2θ equal to 28.75, 32.05, 41.25, 49.55, and 56.25° corresponding respectively to the crystal planes $\left(\bar{1}\,11\right)$, (111), $\left(21\bar{1}\right)$, (220), and (130) of monoclinic ZrO_2 phase, according to JCPDS card No. 37-1484 [38]. While the other sharp peaks that appeared at 29.55, 34.05, 43.75, 48.75, and 57.85° are assigned respectively to the crystal planes (222), (400), (440), and (622) of the cubic Y_2O_3 phase, according to JCODS card No. 89-5591 [39].

It has been reported that the decrease in the intensity of the EPR characteristic peaks upon incorporating NPs makes the sample more rigid with improved mechanical characteristics [40]. The results of the XRD analysis in this study back up the findings in the mechanical characterization of all systems. As a result, a structural investigation is required to comprehend the mechanical properties of polymer nanocomposites.

4. Conclusions

Systematic mechanical property characterizations of EPR incorporated with different concentrations of MWCNT, ZrO_2, and Y_2O_3 NPs were conducted to improve the mechanical properties of the matrix. Results show that the mechanical properties of EPR composites are enhanced effectively by the addition of fillers. For instance, the tensile strength of 0.1% MWCNT filled EPR composites increased by 23%, and Young's modulus increased by 28% in comparison with pure EPR. The highest toughness value of $184.46{\cdot}10^4$ $J.m^{-3}$ is achieved in EPR + ZrO_2 + Y_2O_3 at 0.5 wt.% NPs loading. To design a strong and stiff hybrid PNCs system, the high property mismatch between the NPs and the EPR matrix should reduce by incorporating MWCNT into the matrix, to facilitate the interfacial load transfer mechanism. Therefore, the presence of the MWCNTs in the EPR matrix could make PNCs not only stronger but also tougher.

Declarations

Conflicts of Interest

The authors declare no conflicts of interest.

Acknowledgments

The authors gratefully acknowledge the support and facility of the University of Sulaimani, and the University of Halabja.

References

1. A. Kumar, K. Sharma, A.R. Dixit, A review on the mechanical properties of polymer composites reinforced by carbon nanotubes and graphene. Carbon Lett. **31**, 149–165 (2021)
2. A.H. Mohamad, O.G. Abdullah, S.R. Saeed, Effect of very fine nanoparticle and temperature on the electric and dielectric properties of MC-PbS polymer nanocomposite films. Results in Physics **16**, 102898 (2020)
3. A.K.T. Lau, D. Hui, The revolutionary creation of new advanced materials – carbon nanotubes composites. Compos. Part. B-Eng **33**, 263–277 (2002)
4. R. Ramlee, M. Mariatti, Z.A. Mohd Ishak, A.R. Mohamed, Properties of Glass Fiber-Carbon Nanotube (CNT)/ Epoxy Composites. J. Polym. Mater. **30**, 103–116 (2013)

5. N. Gupta, S.M. Gupta, S.K. Sharma, Carbon nanotubes: synthesis, properties and engineering applications. Carbon Lett. **29**, 419–447 (2019)
6. L.R. Xu, V. Bhamidipati, W.H. Zhong, J. Li, C.M. Lukehart, E. Lara-Curzio, K.C. Liu, M.J. Lance, Mechanical property characterization of a polymeric nanocomposite reinforced by graphitic nanofibers with reactive linkers. J. Compos. Mater. **38**, 1563–1582 (2004)
7. Y. Zare, K.Y. Rhee, Expression of normal stress difference and relaxation modulus for ternary nanocomposites containing biodegradable polymers and carbon nanotubes by storage and loss modulus data. Compos. B Eng. **158**, 162–168 (2019)
8. A.O. Okonkwo, P. Jagadale, J.E.G. Herrera, V.G. Hadjiev, J.M. Saldana, A. Tagliaferro, F.C.R. Hernandez, High-toughness/low-friction ductile epoxy coatings reinforced with carbon nanostructures. Polym. Test. **47**, 113–119 (2015)
9. P. Smolen, T. Czujko, Z. Komorek, D. Grochala, A. Rutkowska, M. Osiewicz-Powezka, Mechanical and electrical properties of epoxy composites modified by functionalized multiwalled carbon nanotubes. Materials **14**, 3325 (2021)
10. Y. Zare, K.Y. Rhee, Tensile modulus prediction of carbon nanotubes-reinforced nanocomposites by a combined model for dispersion and networking of nanoparticles. J. Mater. Res. Technol. **9**, 22–32 (2020)
11. M. Pras, J.F. Gerard, L. Golanski, G. Quintard, J. Duchet-Rumeau, Key role of the dispersion of carbon nanotubes (CNTs) within epoxy networks on their ability to release. Polymers **12**, 2530 (2020)
12. S.B. Aziz, O.G. Abdullah, M.A. Brza, A.K. Azawy, D.A. Tahir, Effect of carbon nano-dots (CNDs) on structural and optical properties of PMMA polymer composite. Results Phys. **15**, 102776 (2019)
13. S. Fu, Z. Sun, P. Huang, Y. Li, N. Hu, Some basic aspects of polymer nanocomposites: A critical review. Nano Mater. Sci. **1**, 2–30 (2019)
14. L.S. Schadler, S.C. Giannaris, P.M. Ajayan, Load transfer in carbon nanotube epoxy composites. Appl. Phys. Lett. **73**, 3842–3844 (1998)
15. B. Song, T. Wang, H. Sun, H. Liu, X. Mai, X. Wang, L. Wang, N. Wang, Y. Huang, Z. Guo, Graphitic carbon nitride (g-C_3N_4) interfacially strengthened carbon fiber epoxy composites. Compos. Sci. Technol. **167**, 515–521 (2018)
16. R. Auvergne, S. Caillol, G. David, B. Boutevin, J.P. Pascault, Biobased thermosetting epoxy: Present and future. Chem. Rev. **114**, 1082–1115 (2014)
17. R. Wazalwar, M. Sahu, A.M. Raichur, Mechanical properties of aerospace epoxy composites reinforced with 2D nano-fillers: current status and road to industrialization. Nanoscale Adv. **3**, 2741–2776 (2021)
18. Z. Zhang, N. Zhao, F. Qi, B. Zhang, B. Liao, X. Ouyang, Reinforced superhydrophobic anti-corrosion epoxy resin coating by fluorine–silicon–carbide composites. Coatings **10**, 1244 (2020)
19. K. Yang, S. Wu, J. Guan, Z. Shao, R.O. Ritchie, Enhancing the mechanical toughness of epoxy-resin composites using natural silk reinforcements. Sci. Rep. **7**, 11939 (2017)

20. D. Chen, J. Li, Y. Yuan, C. Gao, Y. Cui, S. Li, H. Wang, C. Peng, X. Liu, Z. Wu, J. Ye, A new strategy to improve the toughness of epoxy thermosets by introducing the thermoplastic epoxy. Polymer **240**, 124518 (2022)
21. Y. Ling, X. Zhang, L. Yan, H. Zhang, Y. Wang, Y. Ge, Z. Chen, Y. Chen, H. Zou, M. Liang, Silicone-grafted epoxy/carbon fiber composites with superior mechanical/ablation performance. Mater. Chem. Phys. **275**, 125283 (2022)
22. B. Qi, S.R. Lu, X.E. Xiao, L.L. Pan, F.Z. Tan, J.H. Yu, Enhanced thermal and mechanical properties of epoxy composites by mixing thermotropic liquid crystalline epoxy grafted graphene oxide. Express Polym. Lett. **8**, 467–479 (2014)
23. L.C. Tang, H. Zhang, S. Sprenger, L. Ye, Z. Zhang, Fracture mechanisms of epoxy-based ternary composites filled with rigid-soft particles. Compos. Sci. Technol. **72**, 558–565 (2012)
24. D. Saravanan, P. Chandramohan, C.R. Raajeshkrishna, C. Sabarinathan, Enhancement of mechanical properties of epoxy hybrid nanocomposites through hybridization of carbon nanotubes and alumina nanoparticles. Dig. J. Nanomater Biostruct **13**, 483–489 (2018)
25. P.C. Ma, S.Y. Mo, B.Z. Tang, J.K. Kim, Dispersion, interfacial interaction and re-agglomeration of functionalized carbon nanotubes in epoxy composites. Carbon **48**, 1824–1834 (2010)
26. P.C. Ma, N.A. Siddiqui, G. Marom, J.K. Kim, Dispersion and functionalization of carbon nanotubes for polymer-based nanocomposites: A review. Compos. Part. A: Appl. Sci. Manuf. **41**, 1345–1367 (2010)
27. T. Wang, B. Song, K. Qiao, Y. Huang, L. Wang, Effect of dimensions and agglomerations of carbon nanotubes on synchronous enhancement of mechanical and damping properties of epoxy nanocomposites. Nanomaterials **8**, 996 (2018)
28. S. Ayyagari, M. Al-Haik, Y. Ren, D. Nepal, Effect of nano-reinforcement topologies on the viscoelastic performance of carbon nanotube/carbon fiber hybrid composites. Nanomaterials **10**, 1213 (2020)
29. M.R. Zakaria, M.H. Abdul Kudus, H.M. Akil, M.Z.M. Thirmizir, Comparative study of graphene nanoparticle and multiwall carbon nanotube filled epoxy nanocomposites based on mechanical, thermal and dielectric properties. Compo Part. B: Eng. **119**, 57–66 (2017)
30. N. Salah, A.M. Alfawzan, A. Saeed, A. Alshahrie, W. Allafi, Effective reinforcements for thermoplastics based on carbon nanotubes of oil fly ash. Sci. Rep. **9**, 20288 (2019)
31. S. Rostam, D.M.T. Mustafa, S.B. Aziz, Investigation of flexural and creep behavior of epoxy-based nano-sized $CaTiO_3$ particles. Results Mater. **9**, 100164 (2021)
32. N. Kadhim, Y. Mei, Y. Wang, Y. Li, F. Meng, M. Jiang, Z. Zhou, Remarkable improvement in the mechanical properties of epoxy composites achieved by a small amount of modified helical carbon nanotubes. Polymers **10**, 1103 (2018)
33. A. Kaushik, P. Singh, G. Verma, Rekha, Morphology, x-ray diffraction and mechanical properties of resol-montmorillonite clay composites. J. Thermoplast Compos. **23**, 79–97 (2010)
34. C. McClory, T. McNally, G.P. Brennan, J. Erskine, Thermosetting polyurethane multiwalled carbon nanotube composites. J. Appl. Polym. Sci. **105**, 1003–1011 (2007)

35. M.F. Uddin, C.T. Sun, Improved dispersion and mechanical properties of hybrid nanocomposites. Compos. Sci. Technol. **70**, 223–230 (2010)
36. A. Atmakuri, A. Palevicius, L. Kolli, A. Vilkauskas, G. Janusas, Development and analysis of mechanical properties of caryota and sisal natural fibers reinforced epoxy hybrid composites. Polymers **13**, 864 (2021)
37. C. Thongchom, N. Refahati, P.R. Saffari, P.R. Saffari, M.N. Niyaraki, S. Sirimontree, S. Keawsawasvong, An experimental study on the effect of nanomaterials and fibers on the mechanical properties of polymer composites. Buildings **12**, 7 (2022)
38. N.C. Horti, M.D. Kamatagi, S.K. Nataraj, M.N. Wari, S.R. Inamdar, Structural and optical properties of zirconium oxide (ZrO_2) nanoparticles: effect of calcination temperature. Nano Express **1**, 010022 (2020)
39. K.J. Jeong, D.S. Bae, Synthesis and characterization of Y_2O_3 powders by a modified solvothermal process. Kor J. Mater. Res. **22**, 78–81 (2012)
40. D.M.T. Mustafa, S. Rostam, S.B. Aziz, A comparative study on structural, morphological, and tensile properties of binary and ternary epoxy resin-based polymer nanocomposites, Adv. Mater. Sci. Eng. 2020 (2020) 7914796

Figures

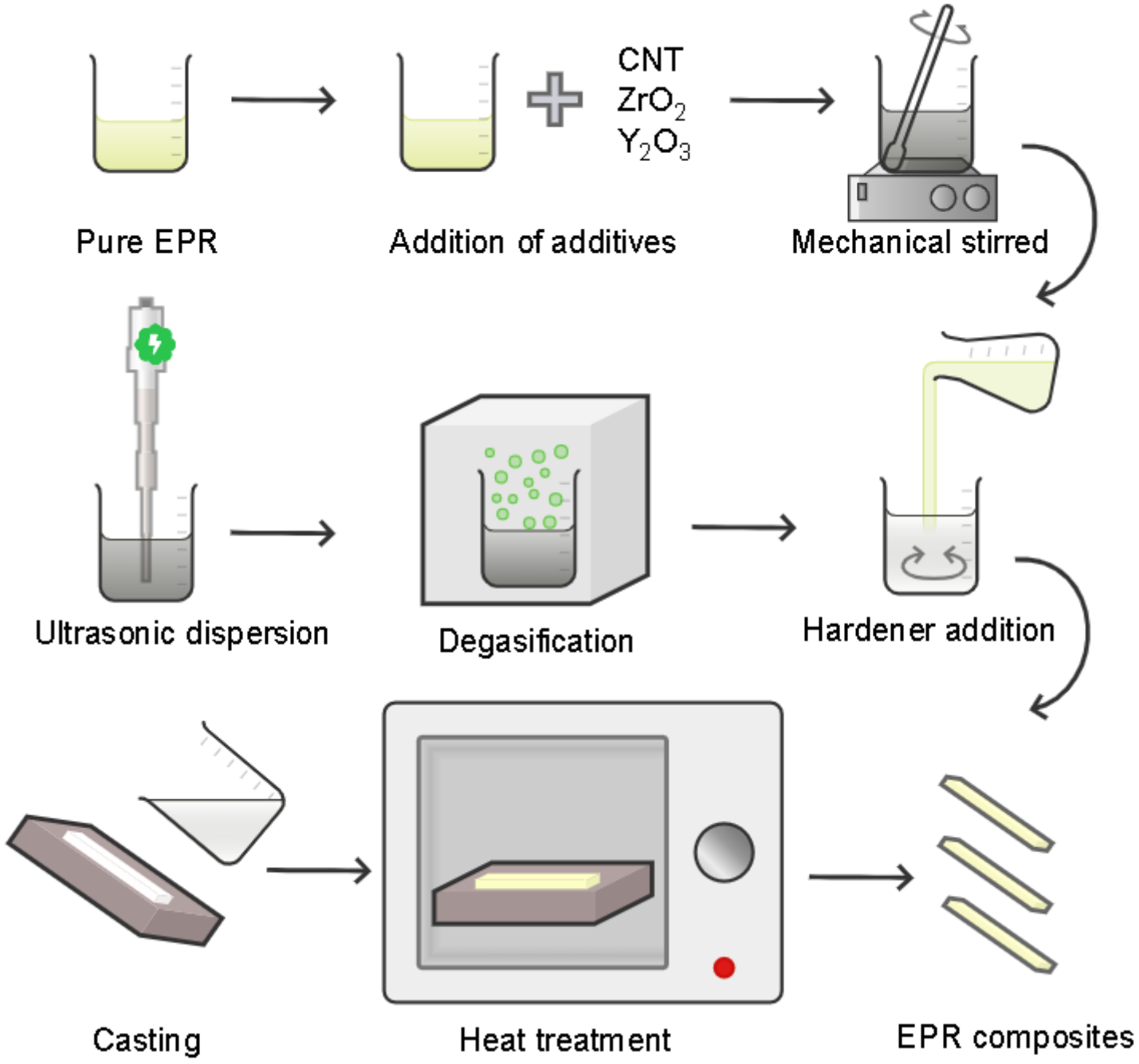

Figure 1

Schematic of the preparation of the EPR nanocomposites.

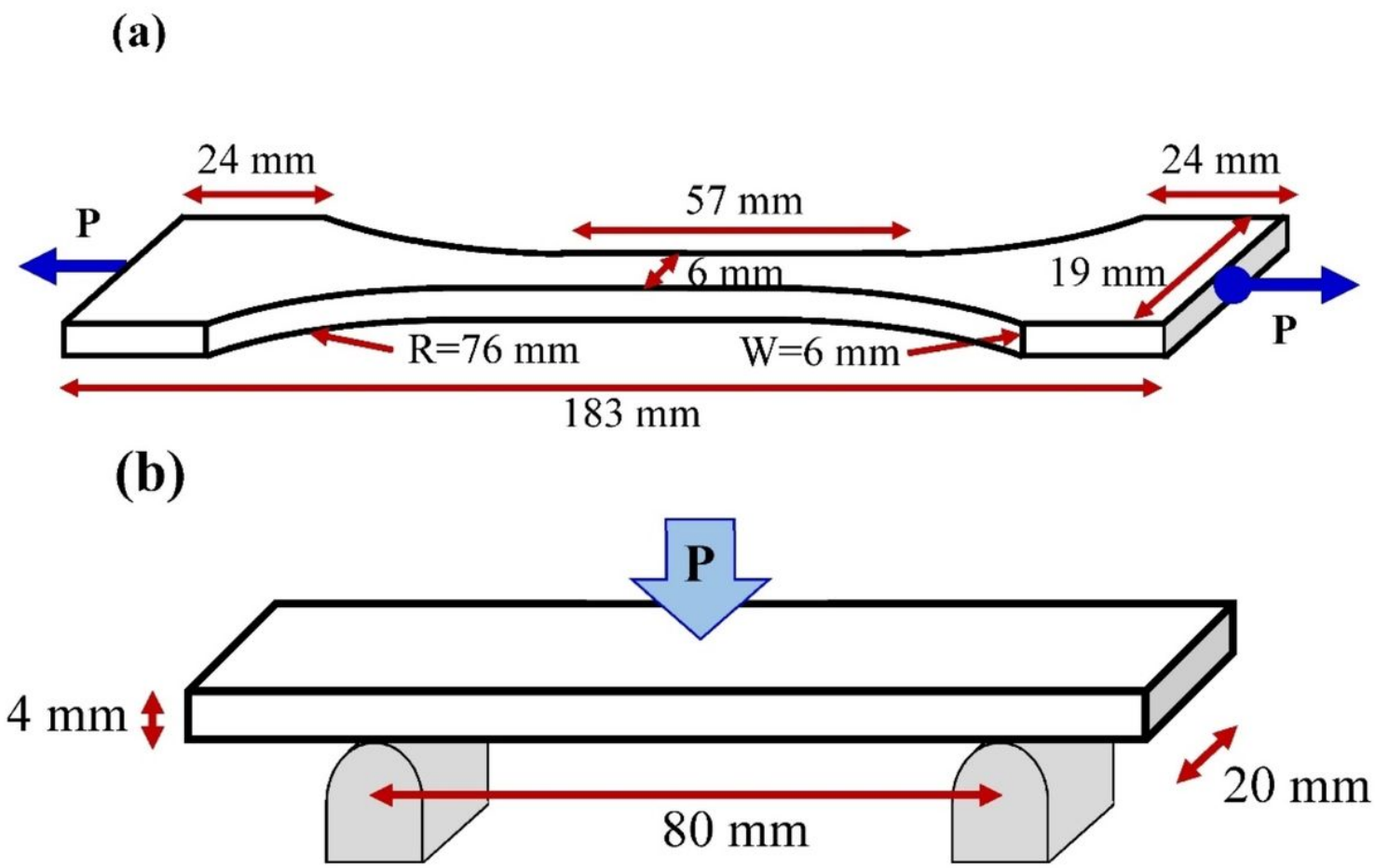

Figure 2

The dimensions of sample and experiment configurations of (a) tensile test, and (b) three-point bend test.

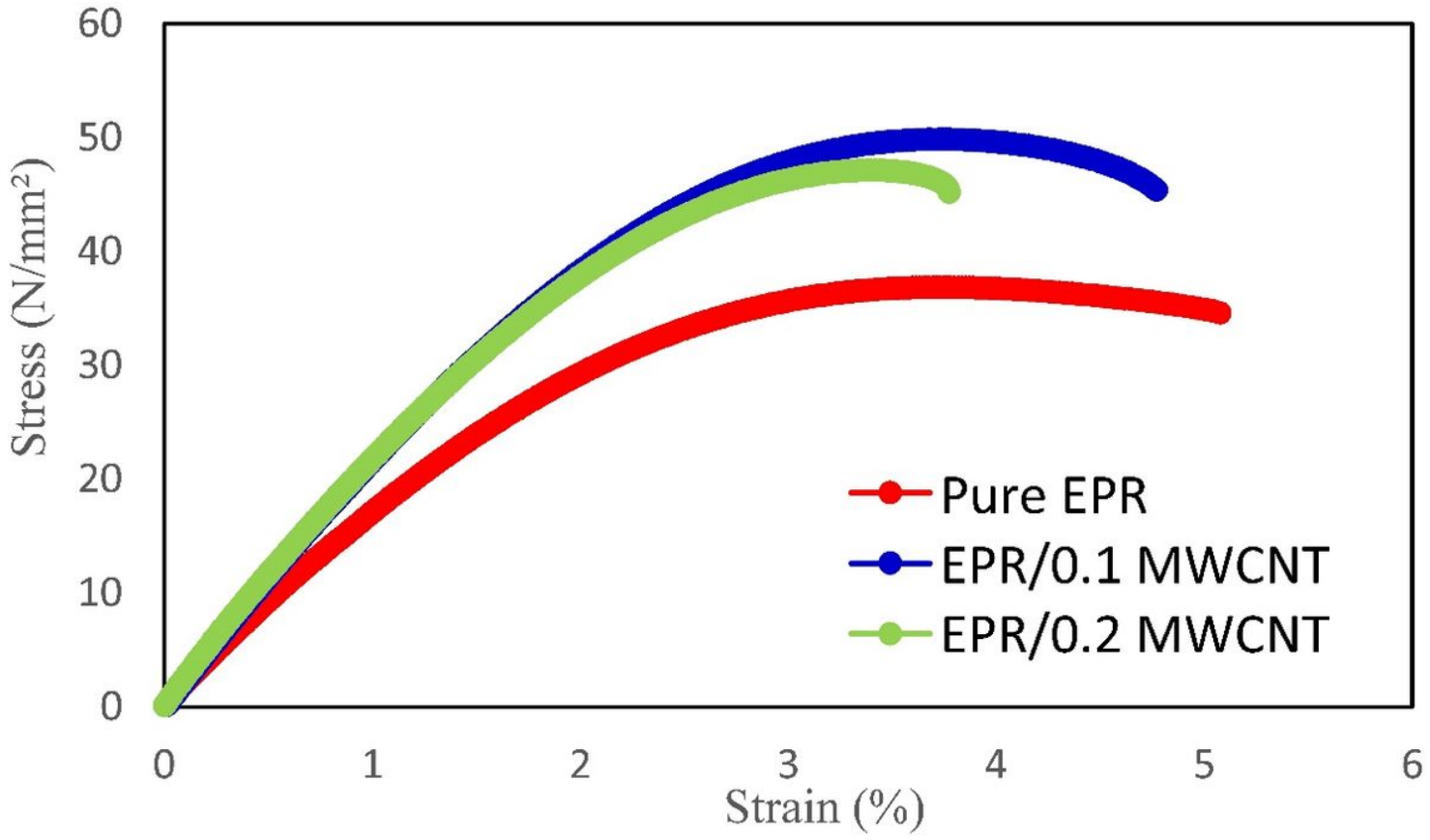

Figure 3

Typical tensile stress-strain curves for pure EPR, and its NCs with different concentrations of MWCNT.

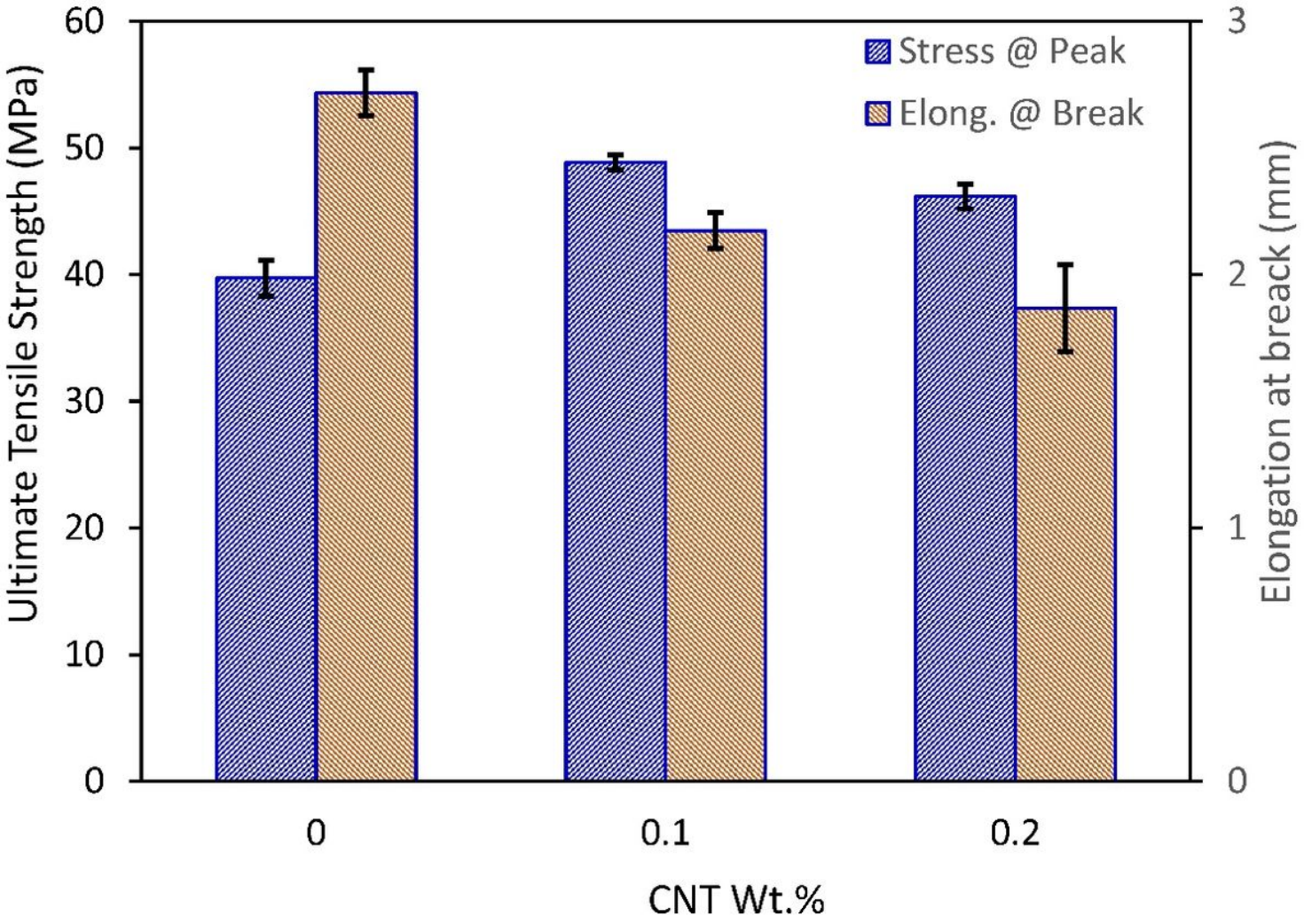

Figure 4

Ultimate strength, and Elongation at break for pure EPR and its PNCs reinforced with MWCNT.

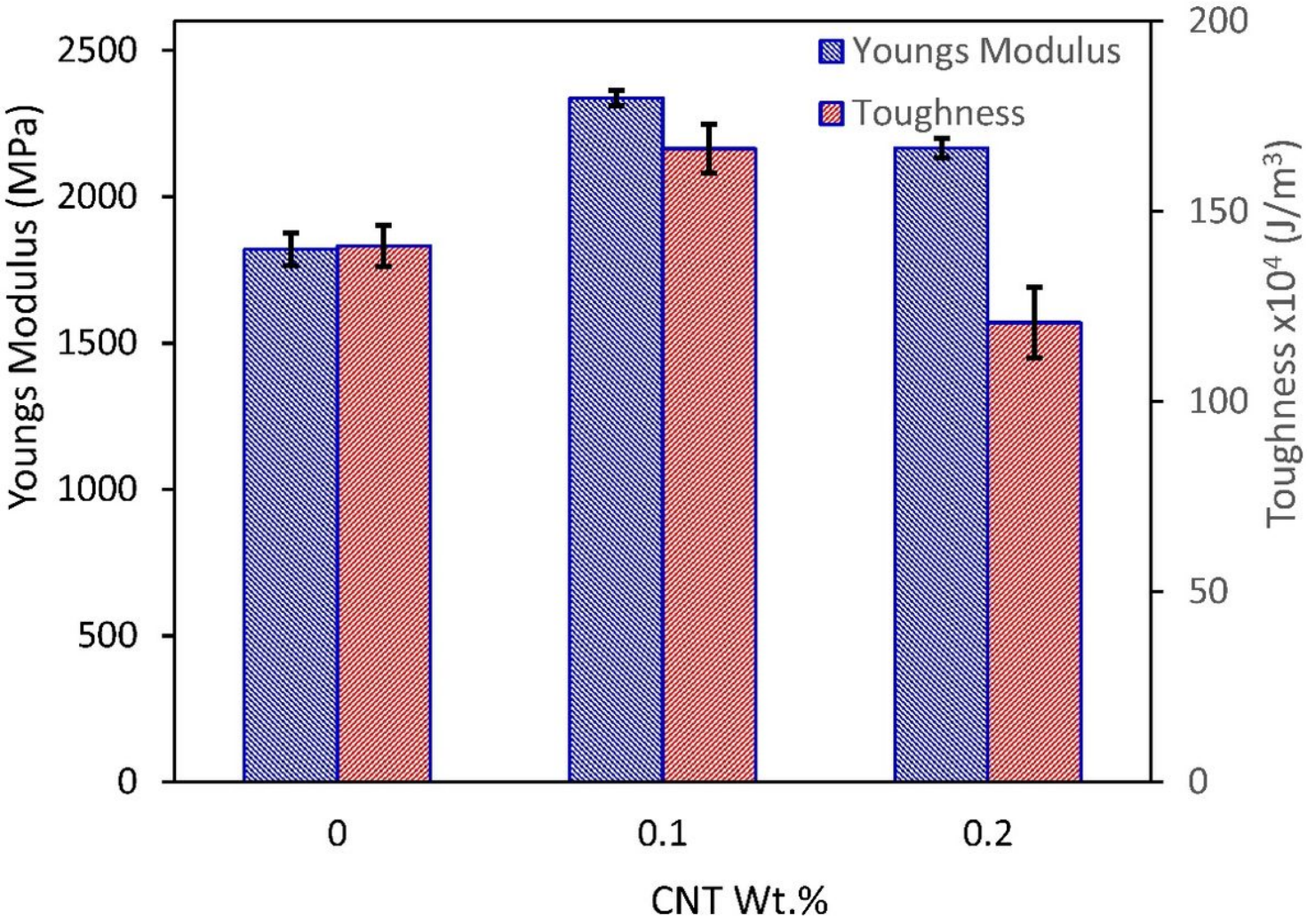

Figure 5

Young's modulus and Toughness for pure EPR and its PNCs reinforced with MWCNT.

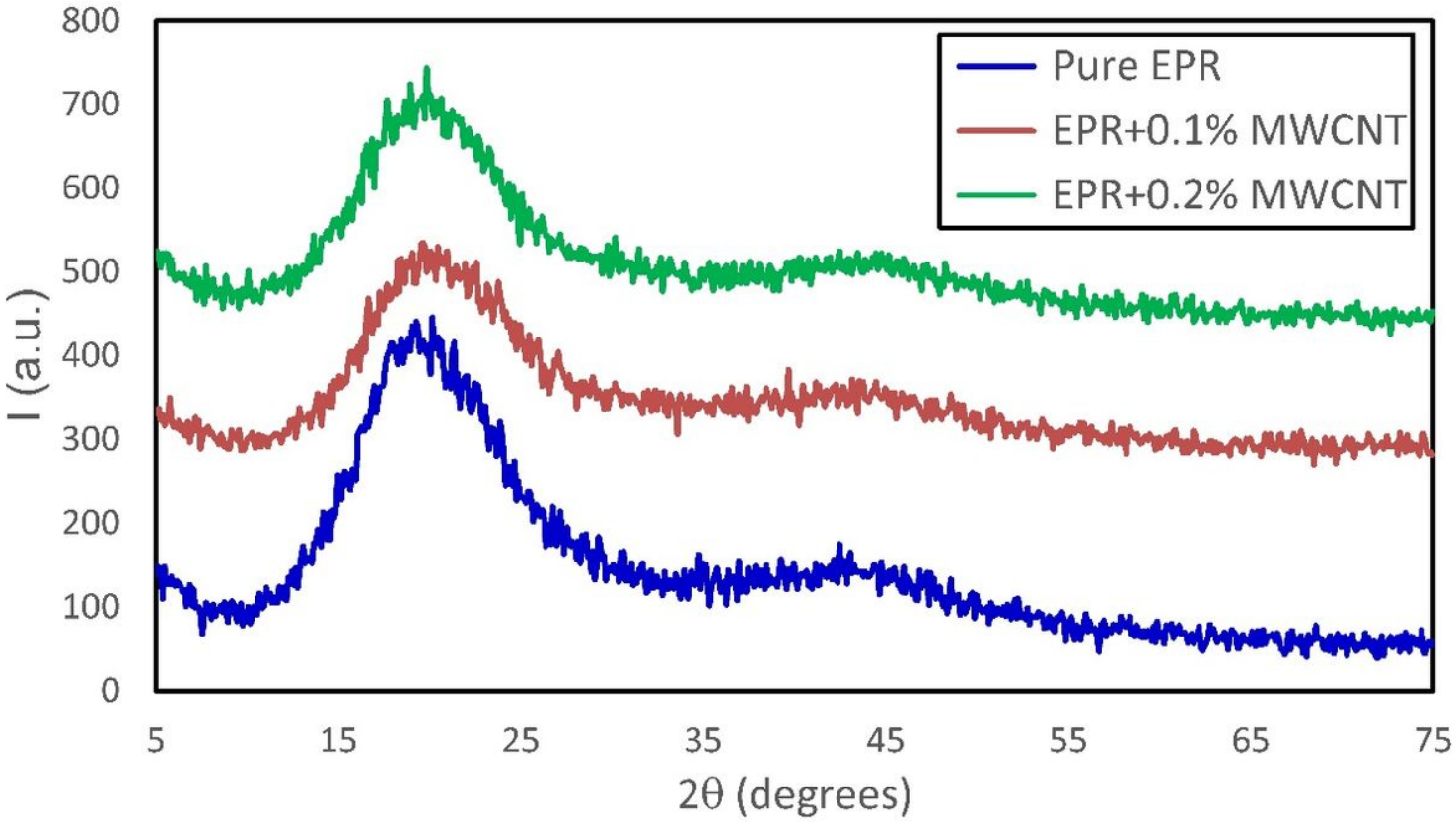

Figure 6

XRD patterns for pure EPR and its PNCs reinforced with 0.1 and 0.2 wt.% MWCNT.

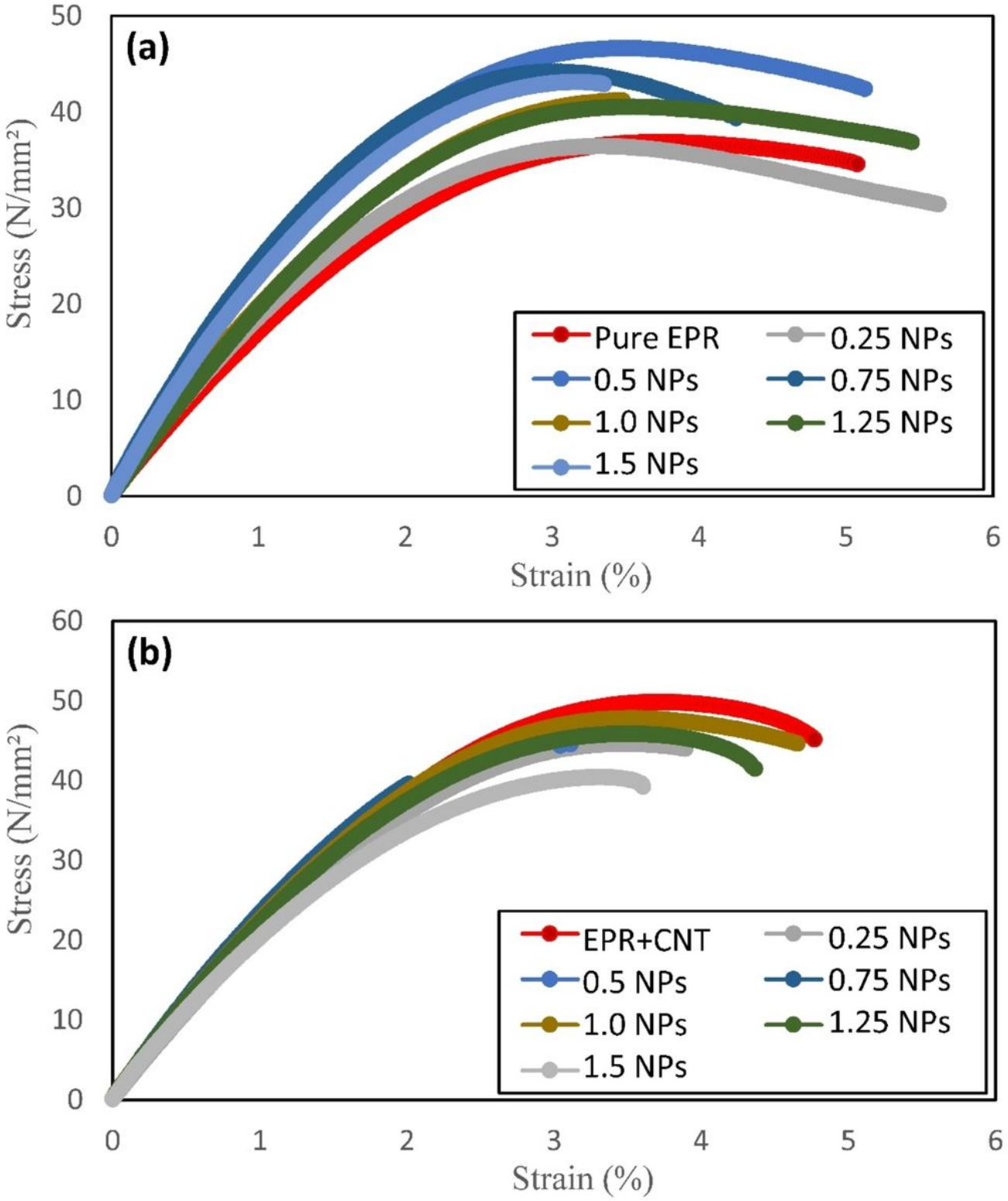

Figure 7

Typical tensile stress-strain curves for (a) EPR PNCs with different concentrations of ZrO_2/Y_2O_3 NPs, (b) EPR/ 0.1 MWCNT PNCs with different concentrations of ZrO_2/Y_2O_3 NPs.

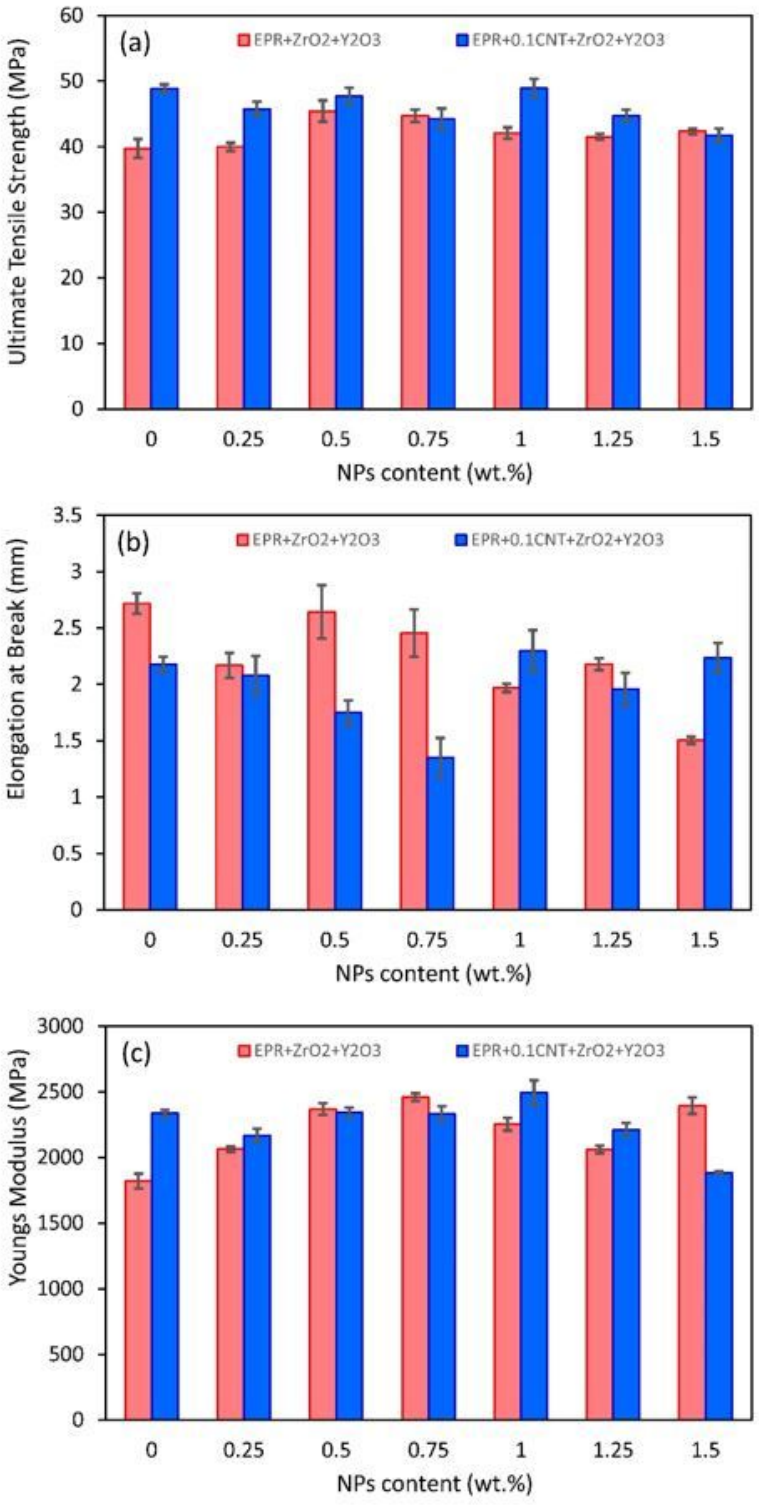

Figure 8

(a) Ultimate strength, (b) Elongation at break, and (c) Young's modulus for all hybrid EPR PNCs.

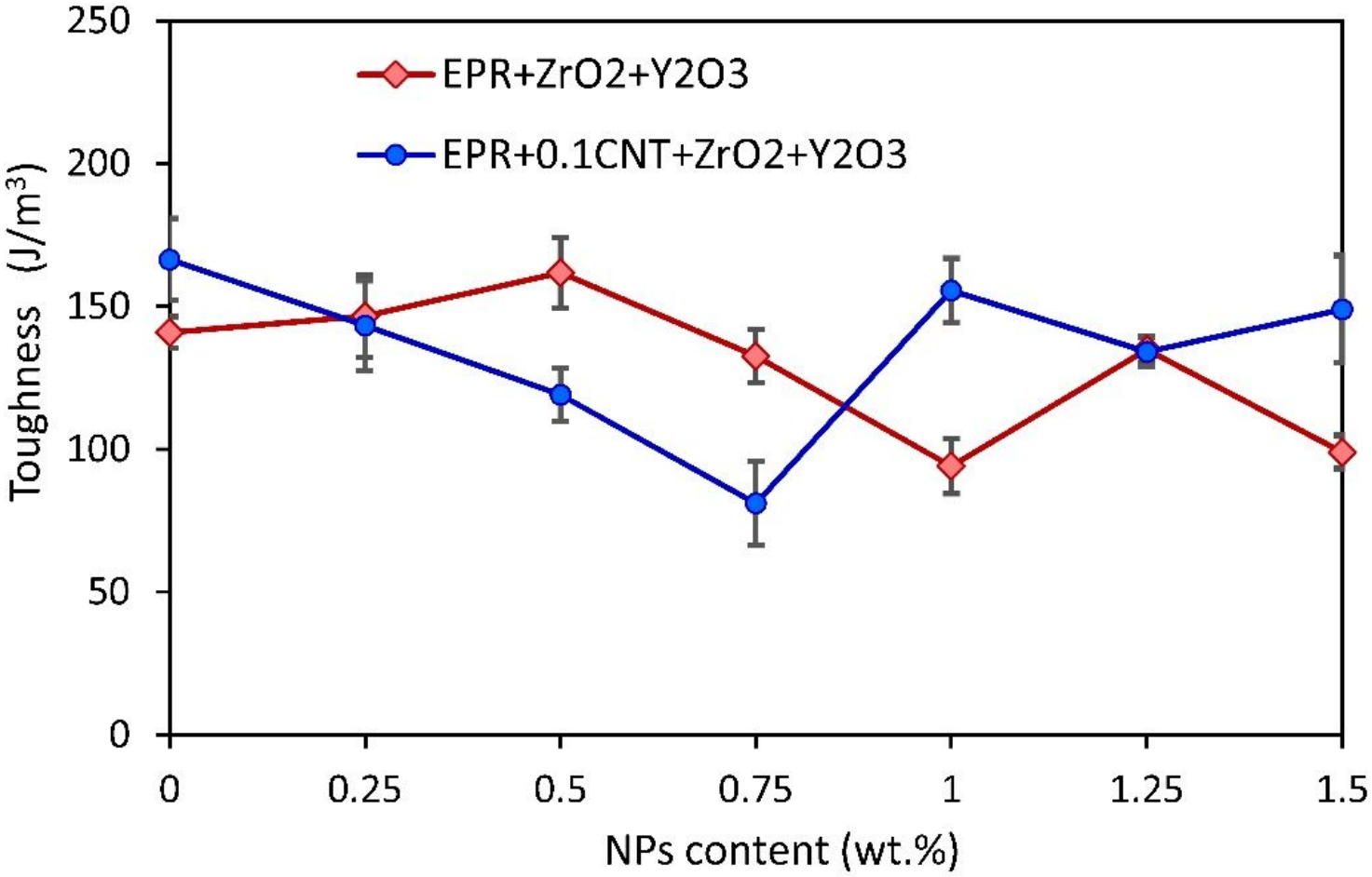

Figure 9

Toughness as a function of NPs content for all hybrid EPR PNCs.

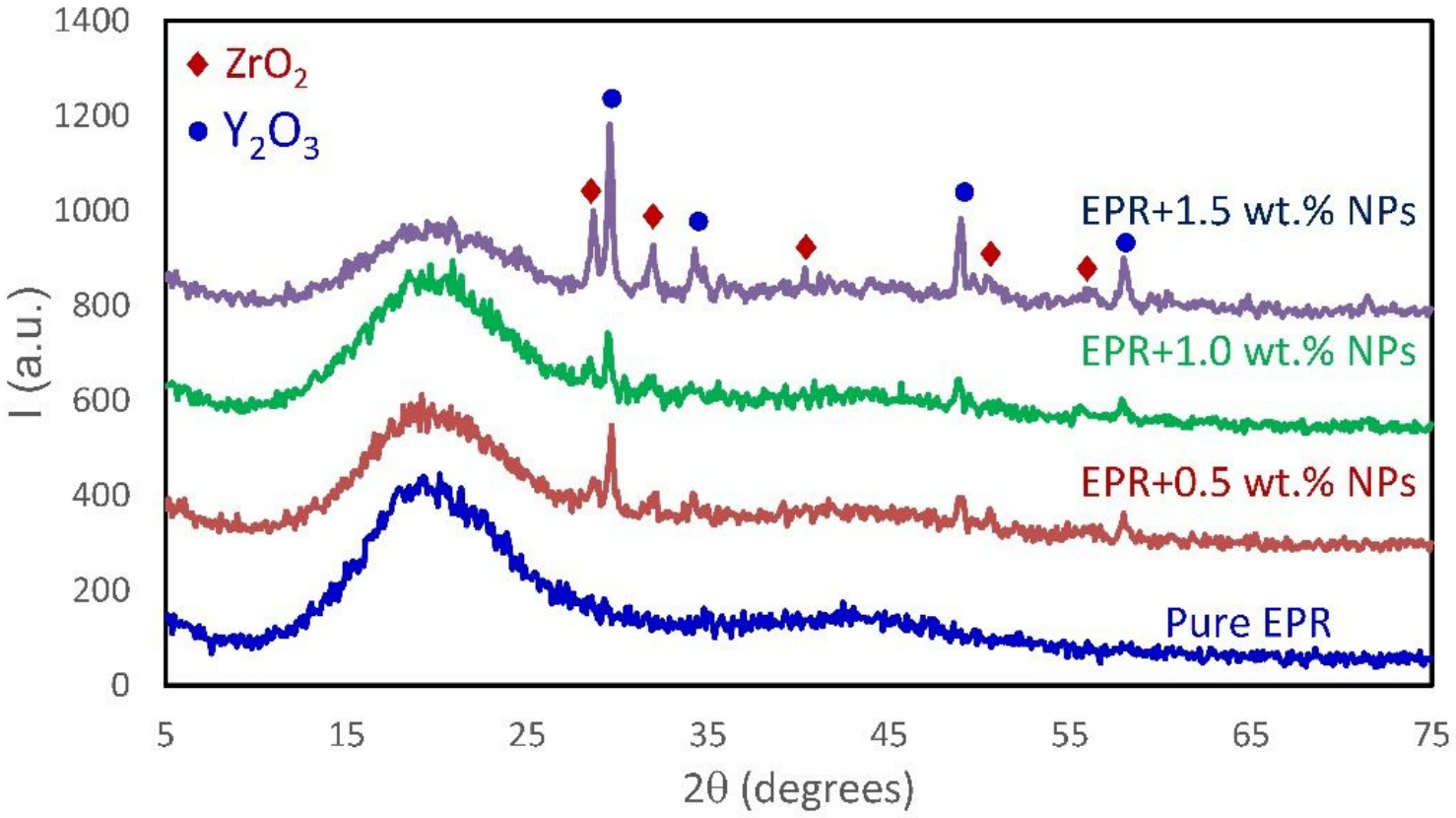

Figure 10

XRD patterns for pure EPR and its hybrid PNCs with different NPs contents.